Binding of the Environmental Pollutant Naphthol to Bovine Serum Albumin

Tuoqi Wu,*,† Qin Wu,*,‡ Shanyue Guan,§ Hengxi Su,‡ and Zejian Cai‡

College of Life Science, Peking University, Beijing, 100871, China, School of Chemical and Energy Engineering, South China University of Technology, Guangzhou, 510641, China, and Instrumental Analysis and Research Center, Sun Yat-sen University, Guangzhou, 510275, China

Received December 14, 2006; Revised Manuscript Received February 26, 2007

The interactions between naphthol and bovine serum albumin (BSA) were investigated by spectroscopy. Our results prove the formation of complex between naphthol and BSA. Hydrophobic interaction dominates in the association reaction. The isomers stack with the aromatic residues in their binding sites with different geometries. Effects of BSA on the excited-state proton transfer and fluorescence spectra of the isomers indicate the different characters of their binding sites. 1-Naphthol inserts deeply into a hydrophobic cavity whereas 2-naphthol is in a basic environment on the surface of BSA. Naphthol statically quenches the fluorescence of BSA in a concentration-dependent manner positively deviating from the linear Stern-Volmer equation. Naphthol binds near Trp-134 in the subdomain IA of the native BSA and is accessible to Trp-212 when BSA is unfolded by naphthol. The folding pattern of the main chain is altered at high naphthol concentration as revealed by the change in the secondary structure. The binding of 1-naphthol is more cooperative than that of 2-naphthol. The extent of cooperativity was estimated by the Hill equation.

Introduction

Naphthalene and its derivatives are industrial materials used in the manufacture of chemical products such as dyes, pharmaceuticals, and synthetics fibers.[1] Naphthol is an important synthetic precursor or degradation product of insecticides.[2,3] Naphthalene and its derivatives are known to be carcinogenic or cocarcinogenic.[4] Naphthalene induces oxidative stress that causes lipid peroxidation and DNA damage in cells and tissues.[5] Toxicity to mononuclear leucocytes and depletion of glutathione were also observed.[6] Naphthalene is metabolized to 1-naphthol and 2-naphthol by P450 isoforms in hepatic microsomes.[7] 1-Naphthol is more cytotoxic than naphthalene.[6] The cytotoxicity and genotoxicity of naphthalene depend on the bioactivation of 1-naphthol.[6] Moreover, 1-naphthol and 2-naphthol can cause depolymerization of spindle microtubules and decrease of protein phosphorylation, which disturb mitotic processing of cells.[8] As a major metabolite of naphthalene, naphthol is an important biomarker for detecting the exposure of humans to polycyclic aromatic hydrocarbons.[7] Fluorescence techniques have been applied to monitor the concentration of naphthol in the urine.[9]

Serum albumin, the most abundant protein in plasma, functions in the binding and transportation of various ligands such as fatty acids, hormones, and drugs.[10] The distribution, free concentration, and metabolism of these ligands strongly depend on their binding constants with serum albumin.[11] Previous studies suggest that the presentation of ligands of albumins to various cells is mediated by the direct interactions between albumin−ligand complex and cell surface, and that such process may involve cell surface receptors.[12] In this sense, both the thermodynamic parameters and the structural information involved in albumin−naphthol interaction are valuable.

Bovine serum albumin (BSA) contains 19 tyrosine and 2 tryptophan residues. The optical properties of them are particular sensitive to the alteration in the tertiary structure. Thus, the absorption and fluorescence spectra can serve to detect the conformational change induced by naphthol binding. Naphthol exists almost completely in its neutral form in the ground state. In the excited state, it becomes more acidic and can deprotonate to produce the anion form in the aqueous solution.[13] The time-resolved fluorescence of the neutral form presents a decay while that of the anion form displays a rise followed by a decay.[13] The rate of excited-state proton transfer (ESPT) and emission properties of naphthol are very sensitive to its local environments.[13] However, to the best of our knowledge, there is no previous study using naphthol as a probe to proteins. In this report, we provide investigations on the effect of naphthol on the structural and optical properties of BSA, the thermodynamic aspects in the binding process, and characters of the binding sites. The results may cast some light on the future study of the interaction between naphthol and other proteins such as enzymes.

Materials and Methods

Materials. 1-Naphthol and 2-naphthol were purchased from Huaqi Chemicals Co., Ltd. Bovine serum albumin was purchased from Sino-American Biotechnology Company (without further purification). For NMR experiments, samples were prepared in 50 mM deuterated phosphate buffer (pH = 7.0). For other experiments, samples were dissolved by Tris-HCl buffer (pH = 7.4).

UV−Visible Spectroscopy. Absorption measurements were performed at room temperature on a U-3010 spectrophotometer (Hitachi). A fixed concentration of BSA (1×10^{-5} M) with various concentrations of naphthol was added to the sample cell. An equal concentration of naphthol was added to the reference cell simultaneously.

Circular Dichroism (CD) Spectroscopy. CD spectra were recorded at 25 °C on a Jasco 810 spectropolarimeter (Jasco) with 0.2 cm path length cylinder cuvettes. The concentration of BSA was fixed at 5×10^{-6} M.

* Corresponding authors. Phone: 86-20-87114377. Fax: 86-20-87114377. E-mail: qwu@scut.edu.cn and tuoqiwu@163.com.
† Peking University.
‡ South China University of Technology.
§ Sun Yat-sen University.

10.1021/bm061189v CCC: $37.00
Published on Web 04/04/2007

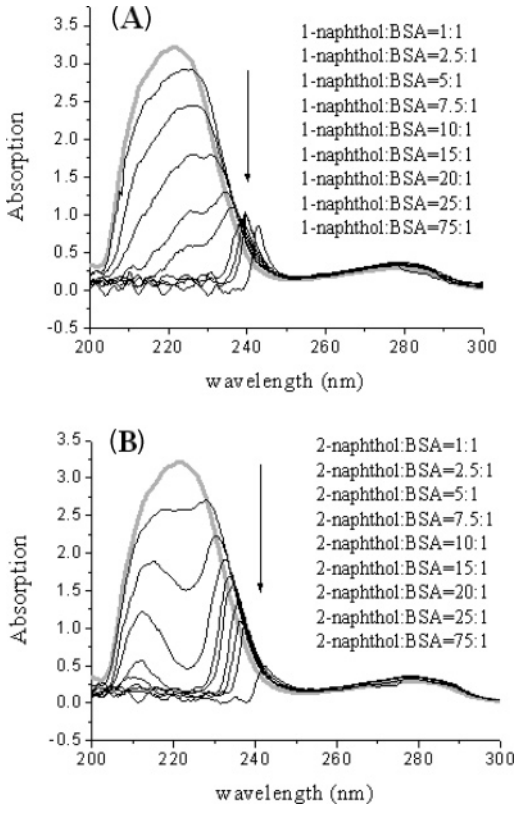

Figure 1. Effect of naphthol on the UV absorption of BSA. The concentration of BSA was fixed at 10 μM. The thick line (gray) is the spectrum of native BSA (10 μM). Thin lines (black) correspond to the spectra of unfolded BSA induced by (A) various concentrations of 1-naphthol and (B) various concentrations of 2-naphthol.

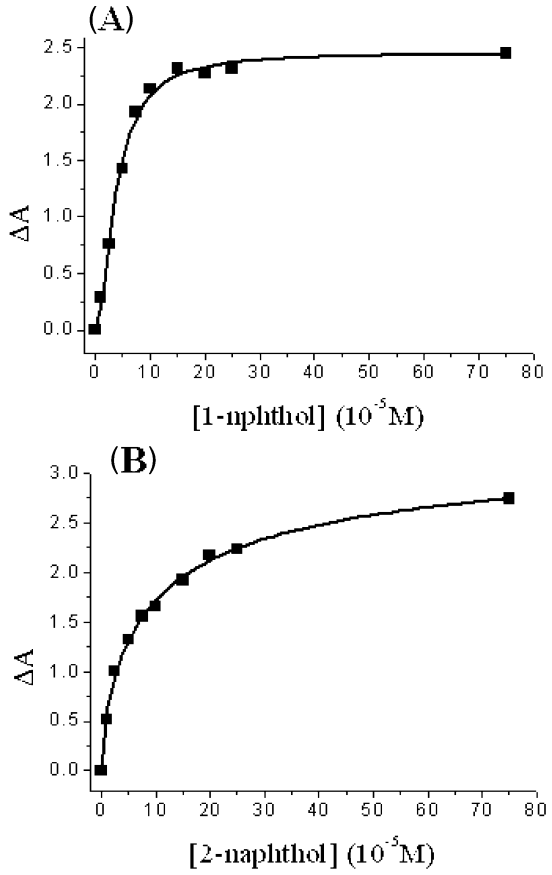

Figure 2. Change in maximum absorbency (ΔA) of BSA versus naphthol concentration. The curves were fitted to the data with the Hill equation. (A) BSA mixed with 1-naphthol. (B) BSA mixed with 2-naphthol.

Steady-State Fluorescence Measurements. The fluorescence profiles were corrected for the wavelength dependence of the sensitivity of the apparatus. Fluorescence spectra were measured on an F-4500 FL Spectrophotometer (Hitachi). Experiments investigating the effect of naphthol on BSA fluorescence were carried out at 25 and 37 °C. An excitation wavelength of 295 nm was applied to selectively excite tryptophan residues. To detect the change in naphthol emission induced by BSA, the excitation wavelength was shifted to 320 nm.

Time-Resolved Fluorescence Measurements. Time-resolved fluorescence experiments were performed at 25 °C on a FLS920 Combined Fluorescence Lifetime and Steady State Spectrometer (Edinburgh Instruments) with 40 kHz lamp frequency. Excitation and emission wavelengths were 295 and 315 nm, respectively, in experiments investigating the fluorescence lifetime of BSA. To determine the fluorescence lifetime of naphthol, the excitation wavelength was shifted to 320 nm and emission wavelength was set at 460 nm for 1-naphthol or 410 nm for 2-naphthol.

NMR Measurements. NMR experiments were carried out on an Avance AV 400 MHz spectrometer (Bruker). The spectra were collected at 25 °C with 32000 data points, 1200 Hz spectral width, 3.4 s acquisition, and 3 s relaxation delay. The spin−lattice relaxation times (T1) were measured with an inversion recovery pulse sequence.

Results and Discussion

UV Absorption Studies. The UV absorption spectrum of BSA shows a weak band in the near-UV region with a maximum at 278 nm and a strong band in the far-UV region with a maximum at 221.5 nm (Figure 1). Binding of naphthol resulted in the decrease of the absorption of BSA in the far-UV region, which is attributed to the exposure of aromatic residues to water.[14] The plots of change in peak value of absorption band ($\Delta A = A - A_0$, A is absorbance at the wavelength where the absorption of unfolded BSA is maximum and A_0 is the absorbance at the wavelength where the absorption of native BSA is maximum) versus naphthol concentration are shown in Figure 2. The data were fitted into the Hill equation. The respective parameters are $n_H = 1.8 \pm 0.2$, $K_{1/2} = 38 \pm 2$ μM for 1-naphthol and $n_H = 0.71 \pm 0.05$, $K_{1/2} = 96 \pm 2$ μM for 2-naphthol. The Hill coefficient of 1-naphthol indicates positive cooperativity, while that of 2-naphthol indicates negative cooperativity. The coefficient can be interpreted as the minimum number of interacting binding sites for naphthol. Thus, the number of sites involved in the cooperative binding of 1-naphthol is at least two.

CD Spectroscopy. The effect of naphthol on BSA stability was investigated by far-UV CD spectra (Figure 3). A high content of α-helices in BSA is revealed by the two minima around 208 and 222 nm.[15] The feature of two minima disappeared when the [naphthol]:[BSA] ratio reached 50 for 1-naphthol or 40 for 2-naphthol (Figure 3). To quantify the content of different types of secondary structures, far-UV CD spectra have been analyzed by the algorithm SELCON3.[16] The tertiary structure class was determined by the CLUSTER program.[17] The values of secondary structures for native and unfolded BSA are shown in Table 1. The tertiary structure class of native BSA was estimated as "all alphas", which is consistent with the crystal structure of its homology, HSA.[18] The protein retained most (>80%) of its helicity until [naphthol]:[BSA] reached 50 for 1-naphthol or 40 for 2-naphthol. A decrease of the α-helices content and an increase of β-strands content were estimated at high naphthol concentration (Table 1). Such tendency was more significant when 2-naphthol was added. The tertiary structure

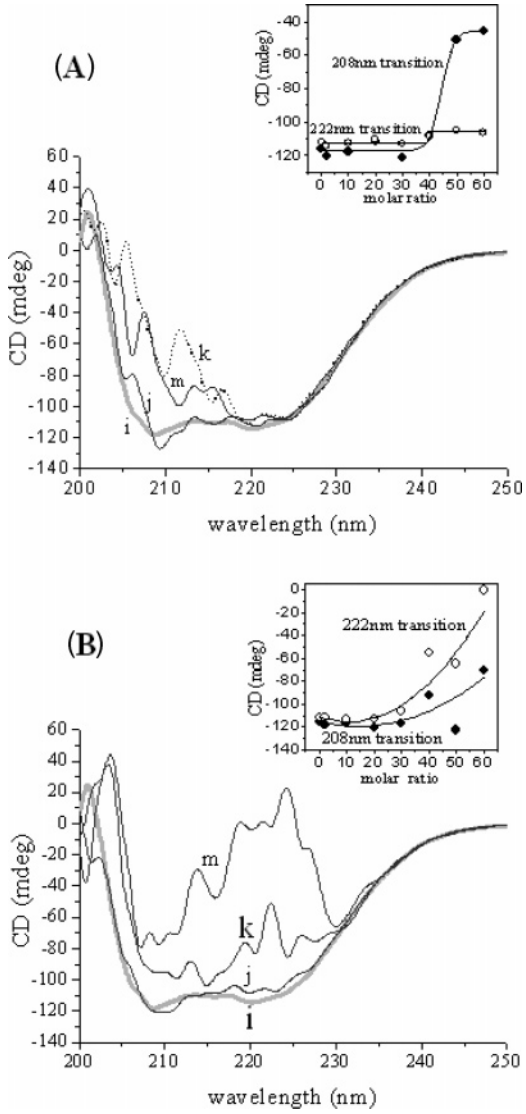

Figure 3. Far-UV CD spectra of BSA (fixed at 5 μM) in the absence and presence of naphthol. (A) CD spectra of (i) native BSA (5 μM) and BSA mixed with 1-naphthol at the molar ratio ([naphthol]:[BSA]) of (j) 40:1, (k) 50:1, (m) 60:1. (B) CD spectra of (i) native BSA (5 μM) and BSA mixed with 2-naphthol at the molar ratio ([naphthol]:[BSA]) of (j) 30:1, (k) 40:1, and (m) 60:1. Insets are the plots of ellipticity at 208 nm (●) and 222 nm (○) versus the molar ratio of naphthol to BSA.

Table 1. Fractions of Different Secondary Structures Determined by SELCON3[a]

substances	molar ratio	H(r) (%)	H(d) (%)	S(r) (%)	S(d) (%)	Trn (%)	Unrd (%)
native BSA		40.1	20.0	2.7	2.9	12.4	21.9
1-naphthol:BSA	40:1	39.5	18.7	2.8	3.0	12.7	23.3
	50:1	24.2	19.5	9.0	6.3	14.0	27.0
	60:1	25.2	19.1	6.3	5.6	15.4	28.4
2-naphthol:BSA	30:1	37.2	20.0	2.5	3.2	13.8	23.4
	40:1	26.2	15.8	8.5	7.1	16.7	25.7
	60:1	20.3	10.0	11.6	9.3	20.4	28.4

[a] H(r): regular α-helix; H(d): distorted α-helix; S(r): regular β-strand; S(d): distorted β-strand; Trn: turns; Unrd: unordered structure.

class of BSA changed from "all alpha" in the native state to "alpha/beta" or "alpha + beta" in the unfolded state.

Quenching of Intrinsic Fluorescence of BSA by Naphthol. BSA contains two tryptophan residues, Trp-134 and Trp-212,

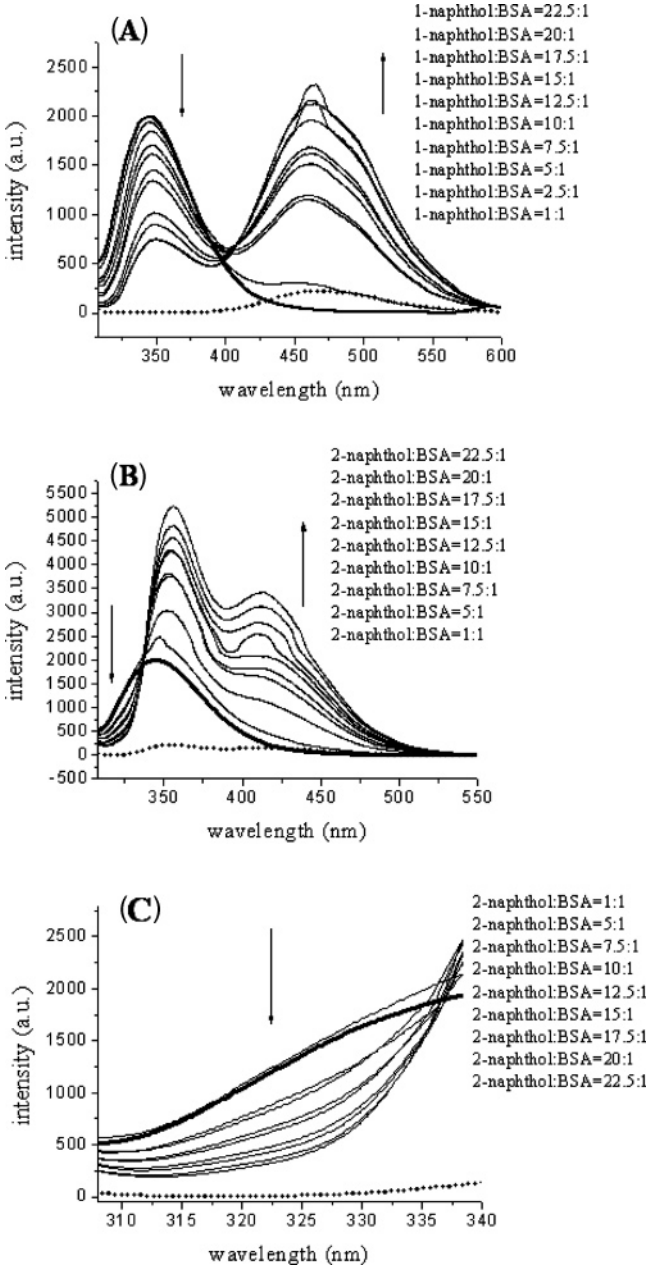

Figure 4. Fluorescence spectra of BSA mixed with various concentrations of naphthol ($\lambda_{excitation}$ = 295 nm) at 25 °C. The concentration of BSA was fixed at 10 μM. Thick line (gray) is the spectrum of native BSA (10 μM). Thin lines (black) correspond to the spectra of the mixture of naphthol and BSA. (A) The spectra of BSA mixed with 1-naphthol. The short dashed line is the spectra of 1-naphthol (10 μM). (B) The spectra of BSA mixed with 2-naphthol. The short dashed line is the spectra of 2-naphthol (10 μM). (C) A concentration-dependent decrease of tryptophan fluorescence was observed on addition of 2-naphthol in the region where the emission of 2-naphthol is negligible.

located in subdomains IA and IIA, respectively.[10] The fluorescence spectrum of BSA presents strong emission with maximum at 344 nm (Figure 4). To exclude the fluorescence of naphthol, the fluorescence signal was monitored as a function of naphthol concentration at 315 nm, where the emission of naphthol is negligible. A concentration-dependent decrease of tryptophan fluorescence was observed (Figure 4).

Time-resolved fluorescence study was applied to investigate the quenching mechanism. There are two lifetime components in native BSA, one (τ_1 = 5.9 ± 0.1 ns) contributing 75.7% of the total fluorescence and the other (τ_2 = 3.2 ± 0.2 ns)

Table 2. Fluorescence Lifetimes (τ) of BSA

sample	molar ratio	τ_1 (ns)	τ_2 (ns)	fraction[a] (%)
native BSA		5.9 ± 0.1	3.2 ± 0.1	75.65
1-naphthol:BSA	1:1	5.9 ± 0.2	3.1 ± 0.2	67.07
	2:1	6.1 ± 0.2	3.1 ± 0.2	58.61
2-naphthol:BSA	1:1	6.1 ± 0.2	3.1 ± 0.2	64.54
	2:1	6.6 ± 0.3	3.2 ± 0.1	48.15

[a] The fraction of fluorescence contributed by the longer lifetime component.

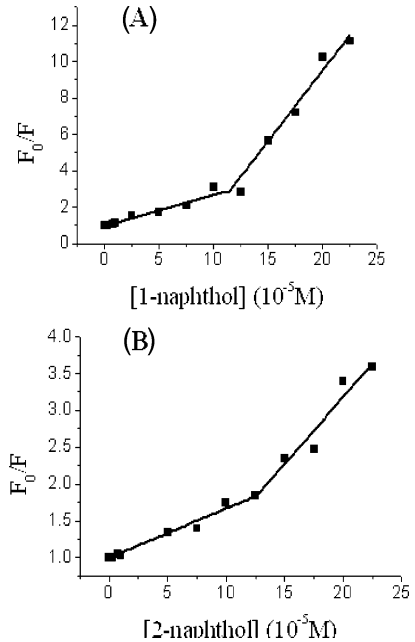

Figure 5. Stern−Volmer plots of tryptophan fluorescence (at 25 °C) quenched by (A) 1-naphthol and (B) 2-naphthol. Lines were fitted to the plots with linear equation.

contributing the rest of the fluorescence (Table 2). The one with a longer lifetime was assigned to Trp-134 and the other was assigned to Trp-212.[19] Addition of naphthol caused a decrease in the fraction of fluorescence contributed by Trp-134 against the total fluorescence of BSA, suggesting that Trp-134 is preferred to be quenched by naphthol (Table 2). It is possible that the binding site of naphthol is near Trp-134. No significant change in τ is observed in the presence of naphthol. Thus, static quenching mechanism is responsible for the observed quenching of tryptophan fluorescence, indicating the existence of a ground state complex between naphthol and BSA.

Fluorescence quenching can be described by the Stern−Volmer equation,

$$\frac{F_0}{F} = 1 + K_q[Q] \tag{1}$$

where F_0 and F are the fluorescence intensities in the absence and in the presence of quenchers, K_q is the quenching constant, and $[Q]$ is the molar concentration of quenchers.[19] Stern−Volmer plots for the quenching of tryptophan fluorescence at 315 nm by naphthol are shown in Figure 5.

1-Naphthol yields a biphasic quenching pattern (Figure 5A). Both phases present a linear dependence on the molar concentration of 1-naphthol. A clear transition was obtained when the molar ratio of 1-naphthol to BSA reached 12. The tryptophan fluorescence decreased by about 70% in the first phase and was almost completely lost in the second phase. Because the two tryptophans in BSA are located in two different subdomains, the results may indicate the presence of at least two 1-naphthol binding sites. Trp-134 is more exposed to the hydrophilic environment while Trp-212 lies in the hydrophobic core.[19] Because of its higher exposure, Trp-134 is more likely to be quenched in the native state, already proved by the time-resolved fluorescence experiments. The first phase of quenching possibly reveals this state. As the concentration of 1-naphthol increased, BSA was unfolded as a result of the hydrophobicity of 1-naphthol. The structure of proteins loosened, forming pores or pathways for naphthol to reach the buried tryptophan. Thus, Trp-212 was exposed to quenchers. As a result, the remaining fluorescence of the first phase was largely quenched. The slope of the Stern−Volmer plots in the second phase is much higher than that in the first phase (Figure 5A). A higher quenching efficiency suggests a larger average exposure of tryptophans to quenchers, which confirms the denaturation of BSA.[20] As shown in CD experiments, the secondary structures of protein were largely unaltered in the same range of molar ratio. Flexible tertiary structure with maintenance of compact main chain implies a molten globule state.[21]

The quenching by 2-naphthol also shows a positive deviation of Stern−Volmer plots from linearity, which indicates the denaturation of BSA and the exposure of buried tryptophan (Figure 5B). However, the biphasic quenching pattern and transition point of 2-naphthol are not as clear as those of 1-naphthol, suggesting that the denaturation process is less cooperative. Considerable fluorescence remained even at high 2-naphthol concentration, which indicates that 2-naphthol quenches the fluorescence of BSA with less effectiveness than 1-naphthol.

From the slopes of Stern−Volmer plots of the two quenching phases of naphthol, the corresponding quenching constants (K_{q1}, K_{q2}) were calculated and listed in Table 3. The quenching constant of 2-naphthol is lower than that of 1-naphthol. A positive dependence of K_q on temperature was observed in the first phase of quenching by naphthol isomers. Assuming the mechanism of quenching is dynamic, the quenching rate constant can be obtained by $k_q = K_{sv}/\tau_0$ ($K_{sv} = K_q$, under such assumption).[22] However, the calculated quenching rate constants for the two naphthol isomers are at a magnitude of 10^{11} M^{-1} s^{-1}, far exceeding the maximum values expected for dynamic quenching of residues in proteins (7×10^9 M^{-1} s^{-1}).[20] Thus, the result proves the static mechanism. The association constants can be obtained by fitting data into the equation[23]

$$F_0 - F = \frac{Q_{max}[Q]}{K_a^{-1} + [Q]} \tag{2}$$

where Q_{max} is the maximum fluorescence that can be quenched and K_a is the association constant for the binding of quencher to BSA. K_a also increased with increasing temperature (Table 3). Thus, the positive dependence of K_q on temperature is due to the increasing affinity of naphthol to BSA. Compared to 1-naphthol, 2-naphthol exhibits less affinity to BSA, which may be responsible for its lower quenching effectiveness. The association constant of 2-naphthol is more influenced by temperature compared to 1-naphthol. Assuming the enthalpy change ($\Delta H°$) does not vary over the temperature range, $\Delta H°$ and entropy change ($\Delta S°$) can be obtained by

$$\ln K_a = -\frac{\Delta H°}{RT} + \frac{\Delta S°}{R} \tag{3}$$

Table 3. Quenching Constants and Thermodynamic Parameters

quencher		K_{q1} ($\times 10^4$ M^{-1})	K_{q2} ($\times 10^4$ M^{-1})	K_a ($\times 10^4$ M^{-1})	$\Delta H°$ (kJ mol^{-1})	$\Delta S°$ (J mol^{-1} K^{-1})
1-naphthol	25 °C	1.6 ± 0.1	8.0 ± 0.8	1.0 ± 0.2	6.7	99
	37 °C	2.15 ± 0.09	7.8 ± 0.4	1.11 ± 0.05		
2-naphthol	25 °C	0.67 ± 0.03	1.8 ± 0.2	0.23 ± 0.06	61	270
	37 °C	1.12 ± 0.04	2 ± 1	0.6 ± 0.1		

where R is the gas constant. As shown in Table 3, both $\Delta H°$ and $\Delta S°$ of the association reaction between naphthol and BSA are positive, which is frequently attributed to hydrophobic interaction.[24]

Effect of BSA on the Emission and ESPT Process of Naphthol. An excitation wavelength of 320 nm where the emission of BSA is negligible was chosen to selectively record the spectra of naphthol (Figure 6). The results of time-resolved experiments are shown in Table 4.

In aqueous solution, 1-naphthol undergoes extremely fast deprotonation, causing a 35 ps lifetime of the neutral emission (~360 nm) and a 35 ps rise time of the anion emission (~460 nm).[13,25] The neutral emission of 1-naphthol in water is too low to be observed due to the extremely short lifetime. On addition of BSA, the peak of neutral emission emerged with a maximum at 354 nm ([naphthol]:[BSA] = 20) and moved to lower wavelength when the concentration of BSA increased (λ_{max} = 349.6 nm for [naphthol]:[BSA] = 1). The emission of anion form underwent a more significant blue shift in the presence of BSA ($\Delta\lambda_{max}$ =15 nm for [naphthol]:[BSA] = 1). The emission of the neutral form was intensified by nearly 50-fold ([naphthol]:[BSA] = 1) and that of the anion form was also enhanced. The increase of neutral emission is due to the retardation of deprotonation.[13] About four water molecules in the neighborhood are needed to solvate the dissociated proton of the excited neutral form.[26] The reduction of the deprotonation rate should be ascribed to the lower polarity of the binding site and lower accessibility of bound naphthol to water molecules. Thus, 1-naphthol is supposed to insert deeply into its hydrophobic cavity on BSA. The blue shift of the anion emission also proves such hydrophobic binding site. Because it is in such an environment, the charged oxygen in the excited state cannot form a hydrogen bond with water molecule to stabilize the excited state as in bulk water. Thus, the emission energy is higher.

Table 4. Time-Resolved Fluorescence Experiments on Naphthol[a]

sample	molar ratio	τ_1 (ns)	τ_2 (ns)	fraction[b] (%)
1-naphthol		6.11 ± 0.02		
	20:1	6.1 ± 0.1	13.8 ± 0.8	24.96
	10:1	5.7 ± 0.1	11.8 ± 0.3	43.02
1-naphthol:BSA	5:1	5.7 ± 0.2	11.4 ± 0.3	48.34
	2:1	6.0 ± 0.2	11.7 ± 0.4	45.67
	1:1	5.7 ± 0.2	11.5 ± 0.3	53.07
2-naphthol		4.5 ± 0.2	9.30 ± 0.08	
	20:1	3.8 ± 0.2	9.11 ± 0.07	
	10:1	3.2 ± 0.2	9.41 ± 0.06	
2-naphthol:BSA	5:1	3.3 ± 0.2	9.52 ± 0.05	
	2:1	3.0 ± 0.2	9.52 ± 0.05	
	1:1	3.0 ± 0.2	9.44 ± 0.05	

[a] For 1-naphthol: τ_1 and τ_2 are the shorter lifetime and the longer lifetime of the anion emission, respectively. As the precision of our time-resolved experiment is on the nanosecond scale, the rise time of 1-naphthol (on the pecosecond scale) is difficult to detect. For 2-naphthol: τ_1 and τ_2 are the rise time and the lifetime of the anion emission, respectively. [b] The fraction of fluorescence contributed by the new lifetime component of 1-naphthol.

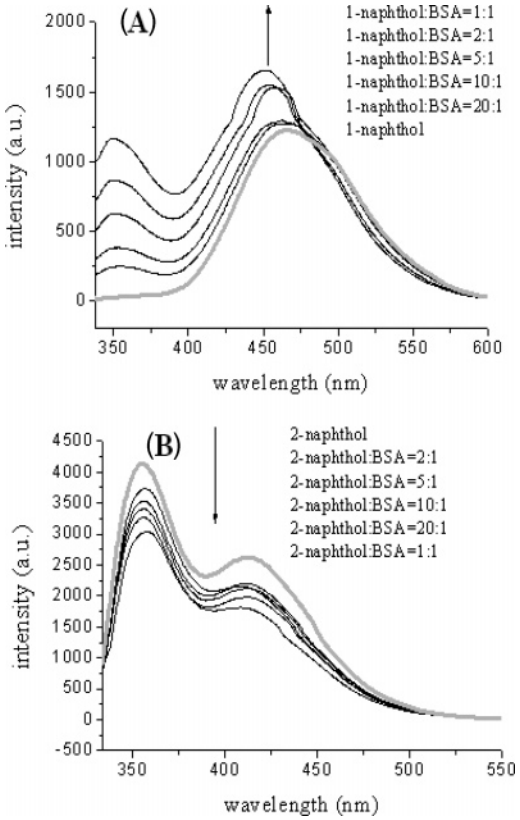

Figure 6. Fluorescence spectra of naphthols with various concentrations of BSA ($\lambda_{excitation}$ = 320 nm, T = 25 °C). The concentration of naphthol was fixed at 1 × 10^{-4} M. Thick lines (gray) are the spectra of naphthols (1 × 10^{-4} M). Thin lines (black) are the spectra of naphthol in the presence of different concentrations of BSA. (A) The spectra of 1-naphthol. (B) The spectra of 2-naphthol. (The peak at shorter wavelength is attributed to neutral emission and the peak at longer wavelength is attributed to anion emission.)

The lifetime of the anion emission of 1-naphthol is 6.11 ± 0.02 ns. On addition of BSA, a new component can be observed with a lifetime of 11.5 ± 0.3 ns ([naphthol]:[BSA] = 1:1). The long lifetime is due to reduction of nonradiative rate, indicating a new environment shielded from the polar solvent.[27] Such conclusion is consistent with the observation in the steady-state experiments. The enhancement of emission near 460 nm is due to the increase in lifetime when naphthol moved from water to the binding site on BSA. The lifetime of the new component did not change significantly at molar ratios below 10 ([naphthol]:[BSA]) and rose to 13.8 ± 0.8 ns at the molar ratio of 20. As discussed above, 1-naphthol bound to the hydrophobic core of BSA at this ratio. The more nonpolar environment leads to further increase in the lifetime of the bound naphthol.

The deprotonation process of 2-naphthol is much slower than that of 1-naphthol. The rise time of the anion emission of 2-naphthol is 4.5 ± 0.2 ns. The neutral form (355.6 nm) exhibits a stronger emission than the anion form (411.2 nm). On addition of BSA, the emission of the neutral form red-shifted (2.4 nm

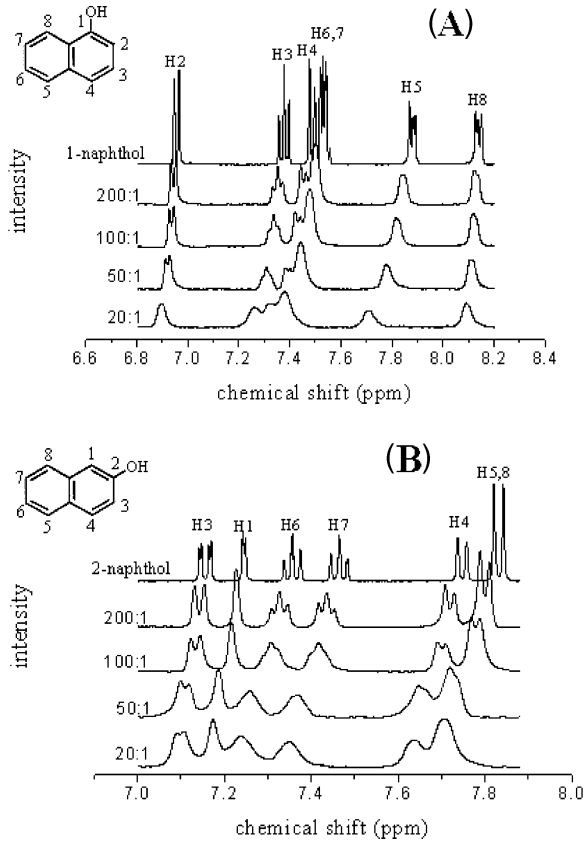

Figure 7. ^{1}H NMR spectra of naphthol at different molar ratios of naphthol (fixed at 2.0×10^{-3} M) to BSA. Assignments are presented in the topmost spectra. (A) NMR spectra of 1-naphthol and 1-naphthol mixed with BSA. (B) NMR spectra of 2-naphthol and 2-naphthol mixed with BSA.

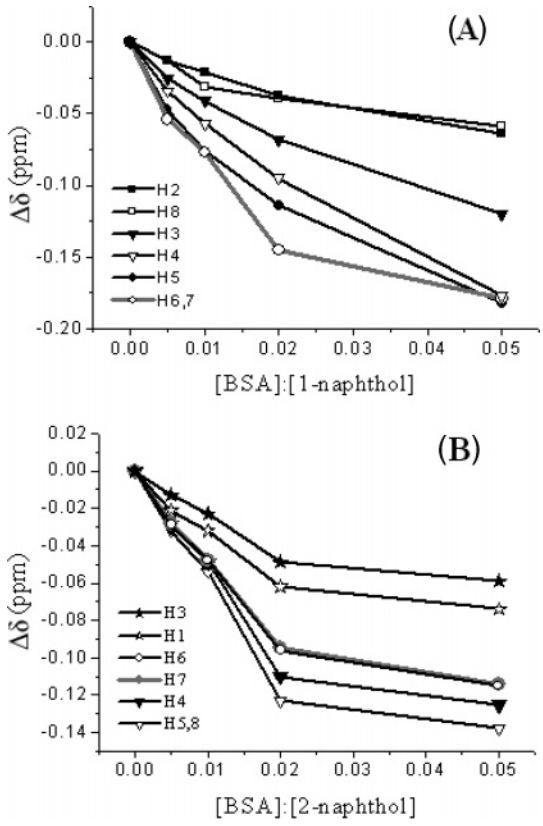

Figure 8. Change in chemical shift ($\Delta\delta$) versus the molar ratio of BSA to naphthol. The binding to BSA induced an upfield shift of proton signals in (A) 1-naphthol and (B) 2-naphthol.

for [naphthol]:[BSA] = 1) while that of the anion form blue-shifted (2.8 nm for [naphthol]:[BSA] = 1). The rise time of the anion emission decreased when BSA was added, indicating an accelerated deprotonation process. The acceleration of deprotonation is due to low proton concentration and high hydroxyl ion concentration in the vicinity of the bound 2-naphthol. Hydroxyl ion, as a hydrogen bond acceptor, favors the conjugation of lone electron pair of hydroxyl oxygen with the aromatic ring,[28] resulting in the red shift of neutral emission. When naphthol loses a proton to form an anion, it cannot establish a hydrogen bond with hydroxyl ion anymore. Repulsion between the two anions raises the energy of the excited state and causes the anion emission to blue shift. The acceleration of deprotonation suggests the availability of bound 2-naphthol to bulk water. Thus, the binding site of 2-naphthol should be located on the surface of BSA. As indicated from a previous study on the binding of 1-aminopyrene to β-cyclodextrin,[29] the bound 2-naphthol may lie in the protein−water interface containing extensive polar groups of BSA, which increase the basicity of surrounding water through hydrogen bonds and facilitate proton dissociation.

The emissions of the two forms decreased in the presence of BSA. The change in lifetime is not comparable to the change in emission intensity. Thus, the loss in emission is more likely due to static quenching. Some quencher of 2-naphthol may lie near the binding site. No new lifetime component of the anion form emerged on addition of BSA. So the polarity of 2-naphthol binding site should be close to that in bulk water.

NMR Spectroscopy. From NMR spectra (Figure 7), it was observed that the chemical shifts and line widths of naphthol changed monotonically with the molar fraction of BSA in the samples. It can be concluded that naphthol undergoes first-order reversible fast exchange between its site on protein and bulk water. All the ^{1}H signals shifted upfield when adding BSA, which indicates $\pi-\pi$ stacking between naphthol and aromatic residues of BSA.[30] Because the average distance between stacked molecules is 0.35 nm and upfield shift falls rapidly with increasing distance of the stacking rings,[31,32] the aromatic residues in the binding site must be very close to the bound naphthol. The upfield shift ($\Delta\delta$) is governed by intermolecular proximity of protons to the aromatic ring and can serve to detect the different environment of protons of the bound naphthol. As shown in Figure 8, protons far from the hydroxyl group upfield-shifted significantly, indicating that they are close to the aromatic ring in the binding site. In contrast, protons near the functional group underwent limited upfield shift. The result suggests that aromatic residue tends to stack with the portion of naphthol far from the OH group, which may be due to the repulsion between the electronegative oxygen and the π cloud of the aromatic ring. According to $\Delta\delta$ of protons, the bound aromatic residue is supposed to bind the edge of 1-naphthol opposite the OH group (center-to-edge or face-to-edge orientation) or the unsubstituted phenyl ring of 2-naphthol (face-to-face orientation). Stacking interaction itself is often too weak to bring two rings together.[33] In fact, bis-naphthyl does not stack in aqueous solution.[34] Thus, the unique environment of binding sites is essential to stacking.

On addition of BSA, the proton signals were broadened and the split peaks arising from spin−spin coupling overlapped into one (Figure 7). Broadening of the signal indicates the decrease of T2 (spin−spin relaxation time) and increase of τ_c (correlation time). To get more insight into the dynamic aspect of binding, quantitative study on T1 was conducted. The correlation time of a small molecule in nonviscous liquid is on the order of 10^{-12} s according to the extreme narrowing condition ($\tau_c \ll 1/\omega_0$).[35]

Table 5. Spin−Lattice Relaxation Time (T1) of Naphthol (Fixed at 2.0×10^{-3} M) in the Absence and Presence of BSA[a]

1-naphthol:BSA	H 2 T1 (s)	H 3 T1 (s)	H 4,6,7 T1 (s)	H 5 T1 (s)	H 8 T1 (s)
50:1	1.435	1.529	1.315	1.951	1.543
200:1	2.168	2.059	1.930	2.070	1.971
1-naphthol	6.418	4.483	4.772	4.505	5.617

2-naphthol:BSA	H 1 T1 (s)	H 3 T1 (s)	H 4 T1 (s)	H 5,8 T1 (s)	H 6 T1 (s)	H 7 T1 (s)
50:1	1.243	1.292	1.309	1.230	1.298	
200:1	2.122	2.200	2.064	2.022	2.008	2.040
2-naphthol	5.715	5.992	4.344	4.187	4.962	4.647

[a] Spin−lattice relaxation times of different protons of naphthol were measured through inversion recovery pulse sequence.

Thus, for naphthol, T1 approaches T2 and decreases with increase in τ_c. As shown in Table 5, T1 of naphthol decreased when BSA was added. For fast exchange, the observed T1 is the weight average of the bound and free naphthol. So T1 of bound naphthol is expected to be much lower. This is due to the fact that when associated with BSA, naphthol exhibited a much larger τ_c proximal to the τ_c of BSA ($\tau_c \sim 41$ ns). Thus, the result confirms that naphthol does indeed complex with BSA.

Effect of Naphthol Binding on BSA Structure. As discussed above, the molten globule state of BSA existed with moderate concentration of naphthol. This state is characterized by the exposure of aromatic side chains and mainly unaltered secondary structure. At higher naphthol concentration, the distribution of different secondary structures of BSA changed, indicating alteration in the folding pattern of the main chain. 1-Naphthol caused a higher cooperative unfolding transition compared to 2-naphthol. This should be attributed to the difference in the position of their binding sites. 1-Naphthol binds deeply in the cavity of BSA, strongly disturbing the hydrophobic core. As a result, nonpolar residues buried in native state are exposed and new hydrophobic sites for 1-naphthol are formed. Such disruption in protein conformation is an all-or-nothing transition.[36] 2-Naphthol, in contrast, binds to the surface of BSA and causes less change in the overall protein structure. Thus, the strength of interaction between different sites is lower. The unfolding of BSA may be due to the perturbation of the solvent shell and depletion of bound water by 2-naphthol resembling the unfolding introduced by alcohols.[37]

Conclusion

The interaction between naphthol and BSA has been investigated by UV, CD, fluorescence, and NMR spectroscopy. Our results prove that naphthol forms a complex with BSA. The fluorescence of BSA is quenched by naphthol through a static quenching mechanism. Naphthol undergoes first-order reversible fast exchange between its binding site on BSA and water. The association constants calculated from fluorescence experiments at 25 °C are $(1.0 \pm 0.2) \times 10^4$ M^{-1} for 1-naphthol and $(2.3 \pm 0.6) \times 10^3$ M^{-1} for 2-naphthol. The affinity of naphthol to BSA increases when the temperature rises. Hydrophobic interaction is involved in the association reaction. When the concentration of naphthol is low, the conformation of BSA is basically unchanged. The bound naphthol is near the Trp-134 residue. So the fluorescence of Trp-134 is preferentially quenched in native state BSA. The binding sites of the two isomers are different. 1-Naphthol lies deep in a hydrophobic cavity shielded from water. Thus, its excited-state proton transfer is retarded and the emission of the neutral form is greatly enhanced. The binding site of 2-naphthol is on the surface of the protein. The microenvironment of bound 2-naphthol is rich in polar amino acid side chains which raise the basicity of the sounding water. Thus, the excited-state proton transfer of 2-naphhthol is accelerated. Moreover, there are quenchers lying near the bound 2-naphthol, which reduce the emission of 2-naphthol. Naphthol interacts with the aromatic residue, in the binding site through $\pi-\pi$ stacking. The geometries of stacking are different for the two isomers. At moderate naphthol concentration, BSA is unfolded. Trp-212 is accessible to naphthol in this state, due to the exposure of aromatic side chains. The unfolding transition induced by 1-naphthol is more cooperative than that induced by 2-naphthol, as a result of their different binding sites. The Hill coefficient indicates that there are at least two binding sites of 1-naphthol on BSA. It is possible that another binding site near Trp-212 is formed in molten globule BSA.

Acknowledgment. This work was supported by Foshan Lianda Textiles Industries Co., Ltd.

References and Notes

(1) Xu, F. X.; Koch, D. E.; Kong, I. C.; Hunter, R. P.; Bhandari, A. *Water Res.* **2005**, *39*, 2358−2368.
(2) Bollag, J. M.; Czaplicki, E. J.; Minard, R. D. *J. Agric. Food Chem.* **1975**, *23*, 85−90.
(3) Crosby, D. G.; Leitis, E.; Winterlin, W. L. *J. Agric. Food Chem.* **1965**, *13*, 204−207.
(4) Xu, Z.; Zhang, Q.; Wu, C.; Wang, L. *Chemosphere* **1997**, *35*, 2269−2276.
(5) Bagchi, M.; Bagchi, D.; Balmoori, J.; Ye, X.; Stohs, S. J. *Free Radical Biol. Med.* **1998**, *25*, 137−143.
(6) Wilson, A. S.; Davis, C. D.; Williams, D. P.; Buckpitt, A. R.; Pirmohamed, M.; Park, B. K. *Toxicology* **1996**, *114*, 233−242.
(7) Cho, T. M.; Rose, R. L.; Hodgson, E. *Drug Metab. Dispos.* **2006**, *34*, 176−183.
(8) Renglin, A.; Olsson, A.; Wachtmeister, C. A.; Önfelt, A. *Mutagenesis* **1998**, *13*, 345−352.
(9) Preuss, R.; Angerer, J. *J. Chromatogr., B: Biomed. Sci. Appl.* **2004**, *801*, 307−316.
(10) Zolese, G.; Falcioni, G.; Bertoli, E.; Galeazzi, R.; Wozniak, M.; Wypych, Z.; Gratton, E.; Ambrosini, A. *Proteins: Struct., Funct., Genet.* **2000**, *40*, 39−48
(11) Kragh-Hansen, U. *Pharmacol. Rev.* **1981**, *33*, 17−53.
(12) Ockner, R. K.; Weisiger, R. A.; Gollan, J. L. *Am. J. Physiol.-Gastrointest. Liver Physiol.* **1983**, *245*, G13−G18.
(13) Mandal, D.; Pal, S. K.; Bhattacharyya, K. *J. Phys. Chem.* **1998**, *102*, 9710−9714.
(14) Donovan, J. W. *J. Biol. Chem.* **1969**, *244*, 1961−1967.
(15) Hong, W.; Jiao, W.; Hu, J.; Zhang, J.; Liu, C.; Fu, X.; Shen, D.; Xia, B.; Chang, Z. *J. Biol. Chem.* **2005**, *280*, 27029−27034.
(16) Sreerama, N.; Woody, R. W. *Anal. Biochem.* **1993**, *209*, 32−44.
(17) Sreerama, N.; Venyaminov, S. Y.; Woody, R. W. *Protein Sci.* **1999**, *8*, 370−380.
(18) Matsuo, K.; Yonehara, R.; Gekko, K. *J. Biochem. (Tokyo)* **2004**, *135*, 405−411.
(19) Patel, A. B.; Srivastava, S.; Phadke, R. S. *J. Biol. Chem.* **1999**, *274*, 21755−21762.
(20) Eftink, M. R.; Ghiron, C. A. *Biochemistry* **1976**, *15*, 672−680.
(21) Ohgushi, M.; Wada, A. *FEBS Lett.* **1983**, *164*, 21−24.
(22) Zhong, W.; Wang, Y.; Yu, J.; Liang, Y.; Ni, K.; Tu, S. *J. Pharm. Sci.* **2004**, *93*, 1039−1046.
(23) Johansson, J. S.; Eckenhoff, R. G.; Dutton, P. L. *Anesthesiology* **1995**, *83*, 316−324.
(24) Ross, P. D.; Subramanian, S. *Biochemistry* **1981**, *20*, 3096−3102.
(25) Webb, S. P.; Yeh, S. W.; Philips, L. A.; Tolbert, M. A.; Clark, J. H. *J. Am. Chem. Soc.* **1984**, *106*, 7286−7288.
(26) Krishnan, R.; Filliagim, T. G.; Lee, J.; Robinson, G. W. *J. Am. Chem. Soc.* **1990**, *112*, 1353−1357.
(27) Lin, S. H.; Lee, S. T.; Yoon, Y. H.; Eyring, H. *Proc. Natl. Acad. Sci. U.S.A.* **1976**, *73*, 2533−2535.

(28) Schulman, S. G. *Fluorescence and Phosphorescence Spectroscopy: Physicochemical Principles and Practice*; Pergamon Press: Oxford, 1977; p 53.
(29) Hansen, J. E.; Pines, E.; Fleming, G. R. *J. Phys. Chem.* **1992**, *96*, 6904−6910.
(30) Sun, H.; Ye, K.; Wang, C.; Qi, H.; Li, F.; Wang, Y. *J. Phys. Chem. A* **2006**, *110*, 10750−10756.
(31) Naumann, C. F.; Prijs, B.; Sigel, H. *Eur. J. Biochem.* **1974**, *41*, 209−216.
(32) Johnson, C. E.; Bovey, F. A. *J. Chem. Phys.* **1958**, *29*, 1012−1014.
(33) Dhar, G.; Bhaduri, A. *J. Biol. Chem.* **1999**, *274*, 14568−14572.
(34) Newcomb, L. F.; Gellman, S. H. *J. Am. Chem. Soc.* **1994**, *116*, 4993−4994.
(35) Becker, E. D. *High Resolution NMR: Theory and Chemical Applications*, 2nd ed.; Academic Press: New York, 1980.
(36) Shakhnovich, E. I.; Finkelstein, A. V. *Biopolymers* **1989**, *28*, 1667−1680.
(37) Deshpande, A.; Nimsadkar, S.; Mande, S. C. *Acta Crystallogr., D: Biol. Crystallogr.* **2005**, *61*, 1005−1008.

BM061189V